# SRCI 구동 유도전동기 시스템의 Angle Control

論 文
37~12~3

# Angle Control for SRCI Fed Induction Motor Drive

金 仁 東*·曺 圭 亨**
(In-Dong Kim · Gyu-Hyeung Cho)

## 요 약

전류원 인버터 구동 유도전동기는 사상한 운전과 휴즈없이 단락 보호가능과 견고함 등으로 인해 산업계에 널리 이용되고 있다. 그러나 전류원 구동 유도전동기 시스템은 부하토오크 변화와 기준속도 변화에 대해 늦은 응답특성과 안정도가 좋지않은 단점을 지니고있다. 그와 같은 단점은 앵글제어 루으프를 추가하므로인해 상당히 개선된다 앵글제어는 인버터형에 따라 달라지는데 본논문에서는 최근에 개발된 동시회생 환류방식 전류원 인버터(Simultaneous Recovery and Commutation Inverter)에 대해 고찰한다.

**Abstract**-The current source inverter-fed induction motor(CSIM) drive is widely used in industry because of its four quadrant operation,fuseless protection, and ruggedness.The CSIM drive system, however, has shortcomins such as slow response and dynamic stability to load torque disturbance and reference speed change. Such a disadvantages can be compensated considerably by means of introducing additional angle angle control loop. The angle control method is dependent upon the inverter type. In this paper, simultaneus recovery and commutation inverter(SRCI) which is developed recently is considered.

## 1. Introduction

The induction motor has many advantages such as rugged structure, low cost, and high ratio of generated torque to inertia. Since its speed is determined by stator frequency, however, an effective speed control is not a simple task comparing with that of DC motor. As the static converter technology is evolved, the inverter-fed induction motor drive is widely used recently for speed control applications. In particular, the current source inverter induction motor drive shown in Fig. 1 is typical of conventional scheme widely used in industry, which is possible to operate on full four quadrants with such a simple control loop[1]. It has ruggged and robust characteristics together with induction motor

*正會員 : 韓國科學技術院 電氣 및 電子工學科 博士課程
**正會員 : 韓國科學技術院 電氣 및 電子工學科 副教授 · 工博
接受日字 : 1987年 11月 5日
一次修正 : 1988年 9月 1日

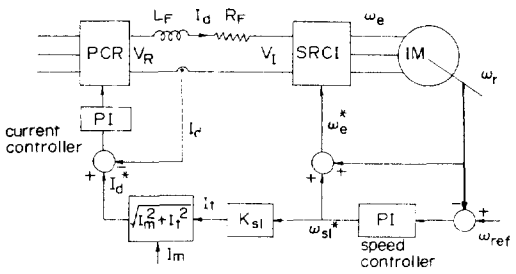


**Fig. 1** Block diagram of CSIM drive.

characteristics.

However, the CSIM drive system has disadvantages such as slow response and poor stability to load torque disturbance and reference speed change. So far, three predominant schemes such as field orientation, synchronous control and angle control scheme are suggested for the control of CSIM drive. Whereas the field orientation and synchronous control scheme have complex structure and require many feedback signals, angle control scheme is simple in structure and easily implemented. All three fast response strategies have common denominator in that they have instantaneous torque angle correction along with the magnitude control of stator current for load torque disturbances and reference frequency change. This aspect is known as frequency compensation. The angle control scheme is thought to be a useful scheme to incorporate the frequency compensation in the simple manner. The distinguishing aspect of the angle controlled CSIM drive is its angle loop or frequency compensation loop. It is reported that, in case of auto-sequentially commutated inverter(ASCI), the performance is enhanced by means of the additional angle control oop.[2] Angle compensation is achieved by considering two terms influenced by the torque angle variation and inverter time delay. The amount of torque angle variation is the same for all kinds of the current source inverters, however, the time delay effect is different depending on the inverter types. Thus the angle control loop should be designed differently. In this paper, recently developed simultaneous recovery and commutation inverter is considered and the angle control method for it is proposed.

## 2. Basic Principle of Angle Control

The term angle is defined to be one between the stator current and magnetizing current in the induction motor, and is generally called "torque angle". In fact, even though there is a case that angle control means to maintain the angle constnt in order to obtain maximum torque per amperes in steady state[3], angle control is generally used to provide fast and stable response for induction motor drive. In the viewpoint of current, angle control means to redistribute the magnetizing current and rotor current, and finally to meet the load torque disturbance. In another viewpoint of flux, angle control is effective to maintain air-gap flux constant even during transient interval.

The angle control method is to add the derivative of the torque angle to the inverter frequency. By doing so, not only the speed of the induction motor can be changed faster but also the required torque is generated faster than the conventional case without angle control, and thus finally the induction motor meets the load torque disturbances effecti vely. In more detail, a simplified equivalent circuit of induction motor is shown in Fig. 2(a), and the corresponding phasor diagram is shown in Fig. 2

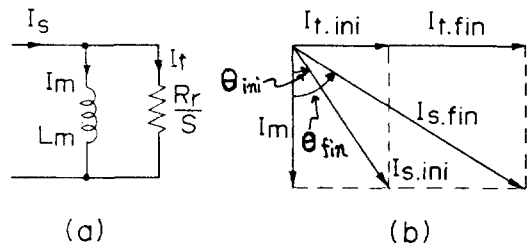


**Fig. 2** Equivalent circuit(a) and phasor diagram (b) of the induction motor.
(a) Simplified induction motor equivalent circuit
(b) Phasor diagram of the motor

(b). When the load torque disturbance is applied, the torque angle begins to increase(or decrease) from its initial state $\theta_{ini}$. In this case if the derivtive portion of the angle is added to inverter frequency,

the motor unit slip increases(or decreases) faster to reduce(or increase) the input impedance of the induction motor faster as well as to increase (or reduce) the torque angle of it faster. It makes the dclink current or motor stator current $I_s$ also increase (or decrease) faster, and thereby the motor reaches its final state($\theta_{fin}$, $I_{s.fin}$, $I_{t.fin}$) faster. Thus fast and stabe response can be obtained in the overall system.

## 3. Inverter Delay and Freouency Variation

SRCI which is used in this paper or angle control is shown in Fig. 3. Looking into the operation of SRCI, the stored energy in the leakage inductance of the motor is transferred to the recovery capacitor during the first part of the commutation. During the second part of the commutation, the energy in the recovery cpacitor is recovered to induction motor itself. This action results in much wider frequency range with much lower device voltage stress compared with the conventional ASCI[4].

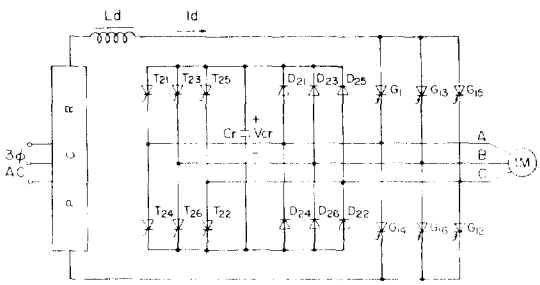


**Fig. 3** Schematic diagram of SRCI inverter.

By analyzing the SRCI commutation operation, the delay time of SRCI is given by

$$T_d = \frac{2L_e I_d}{V_{co} + E_1} \tag{1}$$

where

$L_e$ : leakage inductance of induction motor
$I_d$ : dc link current
$V_{co}$ : recovery capacitor voltage
$E_1$ : back emf of induction motor during commutation interval.

The commutation time delay $T_d$ of SRCI depends on the operating point of the induction motor. Fig. 4 shows $T_d$ as a function of load current for several respective values of inverter frequencies.

The inverter output frequeny variation due to the commutation delay $T_d$ which is dependent upon the operating point can be derived. If the period of the inverter command frequency is denoted to $T_s^*$ as shown in Fig. 5, the period of inverter output frequency is given by

$$T_s = T_s^* + T_s^* \frac{dT_d}{dt} \tag{2}$$

Thus the inverter output frequency $\omega_e$ can be expressed as

$$\omega_e = \frac{2\pi}{T_s} = \frac{2\pi}{T_s^*\left(1 + \frac{dT_d}{dt}\right)} = \frac{\omega_e^*}{1 + \frac{dT_d}{dt}} \tag{3}$$

As $\frac{dT_d}{dt}$ is sufficiently smaller than unity, we obtain

$$\omega_e = \omega_e^*\left(1 - \frac{dT_d}{dt}\right) \tag{4}$$

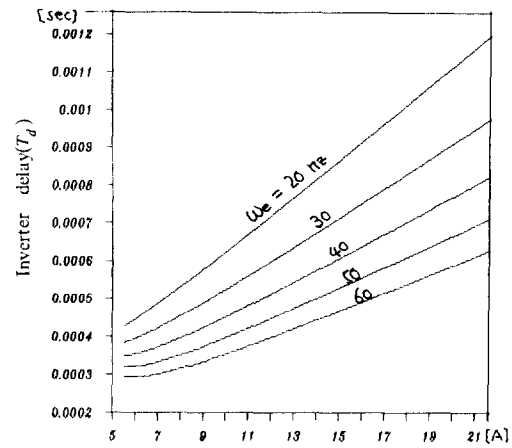


**Fig. 4** Inverter delay($T_d$) .vs. current($I_d$) for five values of inverter frequency($w_e$).

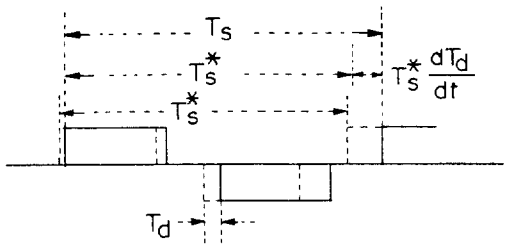


**Fig. 5** Current waveform showing frequency variation due to inverter delay $T_d$ (dashed line : ideal waveform, solid line : delayed waveform by $T_d$).

If $T_d$ is constant reagardless of the operating point of the induction motor, $\omega_e$ becomes equal to $\omega_e^*$. However, $T_d$ is generally dependent upon the operating point and thereby the inverter output frequency is deviated from the inverter command frequency by $-\omega_e^* dT_d/dt$. If the derivative of $T_d$ is positive(negavive) the inverter output frequency decreases(increases) lower(higher) than the inverter command frequency. The unit frequency gain loop including the effect is shown in Fig. 6.

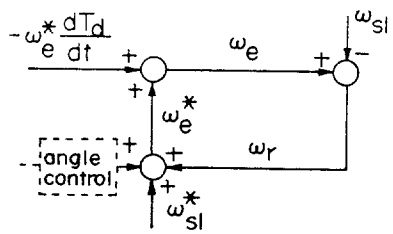


**Fig. 6** Unit gain loop with angle control considering the effect of $T_d$.

In addition, since $\omega_e=\omega_r+\omega_{sl}$ and $\omega_e^*=\omega_r+\omega_{sl}^*$, from (4) we obtain

$$\omega_{sl}=\omega_{sl}^*-\omega_e^*\frac{dT_d}{dt} \tag{5}$$

This equation shows that the actual slip frequency in the induction motor is deviated from the command slip frequency by $-\omega_e^* dT_d/dt$. Thus if the angle control loop is designed without considering the effects of $T_d$, the desired performance can not be obtained. The effect of $T_d$ should be considered and compensated in the angle control loop.

## 4. Proposed Angle Control Method For SRCI

The torque angle in the induction motor is functions of torque producing component $I_t$ and flux producing component $I_m$ of the stator current, and the relation is expressed as

$$\theta=\tan^{-1}\frac{I_t}{I_m} \tag{6}$$

If the air-gap flux of the induction motor is controlled to be constant, the flux prodcing crrent or the magnetizing current is constant. Then the derivative of the control angle becomes

$$\frac{d\theta}{dt}=\frac{d\theta}{dI_t}\frac{dI_t}{dt} \tag{7}$$

where

$$\frac{d\theta}{dI_t}=\frac{I_m}{I_m^2+I_t^2} \tag{8}$$

If the capacitor voltage $V_{co}$ of SRCI is controlled proportional to the inverter frequency with an offset voltage, the inverter commtaion delay can be given by

$$T_d=\frac{2L_eI_d}{k\omega_e+V_{co.offset}+E_1} \tag{9}$$

where

$$I_d=\sqrt{I_t^2+I_m^2}$$

Then, we obtain

$$\frac{dT_d}{dt}=\frac{dT_d}{dI_t}\frac{dI_t}{dt} \tag{10}$$

where

$$\frac{dT_d}{dI_t}=\frac{2L_eI_t}{(k\omega_e+V_{co.offset}+E_1)\sqrt{I_m^2+I_t^2}} \tag{11}$$

From (7) and (10), the amount of frequency added to the inverter frequency for angle control can be

represented by the sum of the two components as

$$\frac{d\theta_{eq}}{dt} = K\frac{d\theta}{dt} + \omega_e^* \frac{dT_d}{dt} \tag{12}$$

where the first term of the right-hand side denotes the compensating qantity of the torque angle and the second term denotes that of the inverter time delay. Thus From (7), (10) and (12), we can write

$$\frac{d\theta_{eq}}{dt} = K_{\theta_{eq}}(I_t, \omega_e^*)\frac{dI_t}{dt} \tag{13}$$

where

$$K_{\theta_{eq}}(I_t, \omega_e^*) = K\frac{d\theta}{dI_t} + \omega_e^* \frac{dT_d}{dI_t} \tag{14}$$

Angle control loop can be designed using equation (13) and can be implemented as shown in Fig 7. The overall block diagram including the loop is shown in Fig. 8. The actual values of each term of equation (14) is shown in Fig. 9 as function of load current for three different values of inverter frequency for 5 Hp induction motor drive. It shows that the effect of commutation delay $T_d$ gradually dominates as the load current increases.

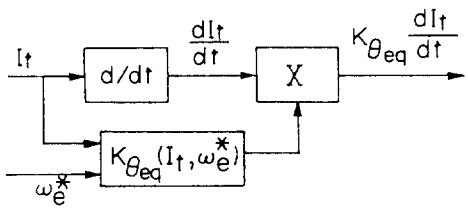


**Fig. 7** Torque angle controller.

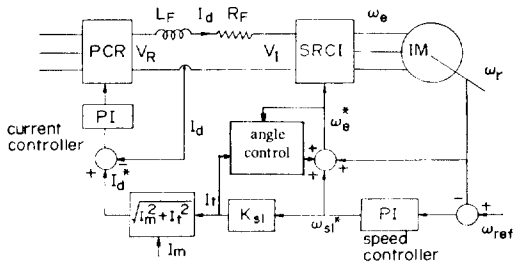


**Fig. 8** Block diagram of angle-controlled SRCI induction motor drive.

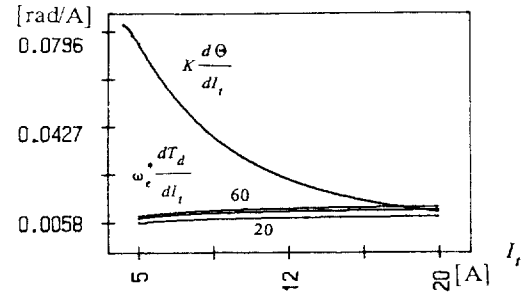


**Fig. 9** $Kd\theta / dI_t$ and $\omega_e^* dT_d / dI_t$ .VS. torque curent ($I_t$) for th ree values of inverter frequency (20Hz, 40Hz, 60Hz).

## 5. Effects of Angle Control on Overall Stability And Dynamic Characteristics

### 5.1 State Equation of Overall System

The state equation describing overall system except speed controller is obtained as shown below by adding the states of the respective blocks to motor equation[5] and including the inverter output frequency variations due to the inverter time delay $T_d$

$$\begin{bmatrix} \frac{X_s+X_F}{\omega_b} & \frac{X_m}{\omega_b} & 0 & 0 & 0 \\ \frac{X_m}{\omega_b} & \frac{X_r}{\omega_b} & 0 & 0 & 0 \\ 0 & 0 & \frac{X_r}{\omega_b} & 1 & 0 \\ 0 & 0 & 0 & 1 & 0 \\ 0 & 0 & 0 & 0 & \frac{2J}{P} \end{bmatrix} \begin{bmatrix} pi_{qs} \\ pi_{qr} \\ pi_{dr} \\ pQ_t \\ p\omega_r \end{bmatrix} +$$

$$\begin{bmatrix} R_s+R_F & 0 \\ 0 & R_r \\ \frac{\omega_e^*\left(1-\frac{dT_d}{dt}\right)-\omega_r}{\omega_b} X_m & \frac{\omega_e^*\left(1-\frac{dT_d}{dt}\right)-\omega_r}{\omega_b} X_r \\ K_i & 0 \\ -\frac{3PX_m i_{dr}}{4\omega_b} & 0 \end{bmatrix}$$

$$\begin{bmatrix} \frac{\omega_e^*\left(1-\frac{dT_d}{dt}\right)}{\omega_b} & X_m & -1 & 0 \\ \frac{\omega_e^*\left(1-\frac{dT_d}{dt}\right)}{\omega_b} - \omega_r & X_r & 0 & 0 \\ R_r & & 0 & 0 \\ 0 & & 0 & 0 \\ 0 & & 0 & \frac{2B}{P} \end{bmatrix} \begin{bmatrix} i_{qs} \\ i_{qr} \\ i_{dr} \\ Q_i \\ \omega_r \end{bmatrix}$$

$$= \begin{bmatrix} 0 \\ 0 \\ 0 \\ \frac{2/3}{\pi} K_t \sqrt{I_m^2 + (K_{sl}\omega_{sl}^*)^2} \\ -T_l \end{bmatrix} \quad (15)$$

where

$$\omega_e^* = \omega_{sl}^* + \omega_r + \frac{d\theta_{eq}}{dt} \quad (16)$$

The third term $d\theta eq / dt$ in expression(16) is additional term for angle control.

### 5.2 Effects of Angle Control on System Stability

The overall system is simply represented in Fig. 10. The loop transfer function of this system can

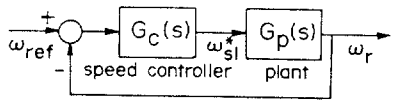


**Fig. 10** Simplified representation of the speed control loop.

be given by $G_C(s)G_P(s)g$ where the part of loop transfer function including variations due to angle control loop is $G_P(s)$. If $G_C(s)$ is defined to be unity, the effects of angle control to the system stability can be shown by the Bode plot of transfer function $G_P(s)$. To plot the Bode diagram, the overall system should be linearized at the operating point, and the transfer function $G_P(s)$ should be obtained. At the operating point $\omega_{ro}$=56.5Hz, $T_l$=10N.m, the gain and phase of transfer function $\omega_r / \omega_{sl}$ is shown in Fig. 11 for both with and without angle control cases. As shown in Fig. 11, phase margin is improved, when angle control is done. In other words, the bandwidth can be increased further for the same phase margin.

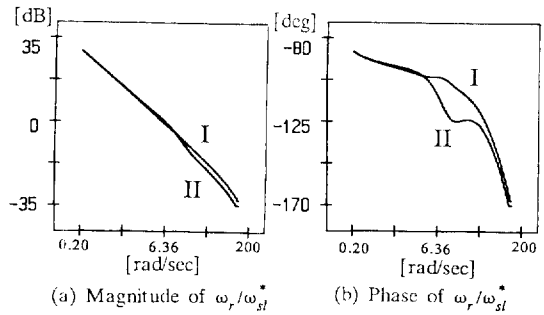


(a) Magnitude of $\omega_r/\omega_{sl}^*$ (b) Phase of $\omega_r/\omega_{sl}^*$

**Fig. 11** Bode plot of CSIM drive for SRCI(I. with angle control, II. without angle control, at $\omega_{ro}$=56.5Hz,$T_l$=10Nm)

### 5.3 Effects of Angle Control on System Dynamics

In order to obtain the transient response, the state of the speed controller is added to the equation(15) and Runge-Kutta method is applied to the resultant equations. Here PI controller is used as speed controller. In Fig. 12, I and Ⅲ show the responses of SRCI and ASCI, respectively, without angle control, Ⅱ shows SRCI response with compensation of the inverter output frequency variation due to $T_d$ only. and Ⅳ shows the response of SRCI with full compensation. It shows that the angle control applied for SRCI provides faster response, lower overshoots and better stability. In addition, the air-gap flux of the induction motor is kept nearly constant even during the transient interval of load torque change.

## 6. Experimental Results

The experiment was performed using the 5 Hp induction motor of which the parameter are

$R_s$=0.45Ω $R_r$=0.47Ω

$L_s$=77.3mH $L_r$=78.9mH

$L_m$=76mH $J$=0.12kg·m²

$B$=0.0082kg·m²/sec

As the inverter, SRCI shown in Fig.3 is used in the

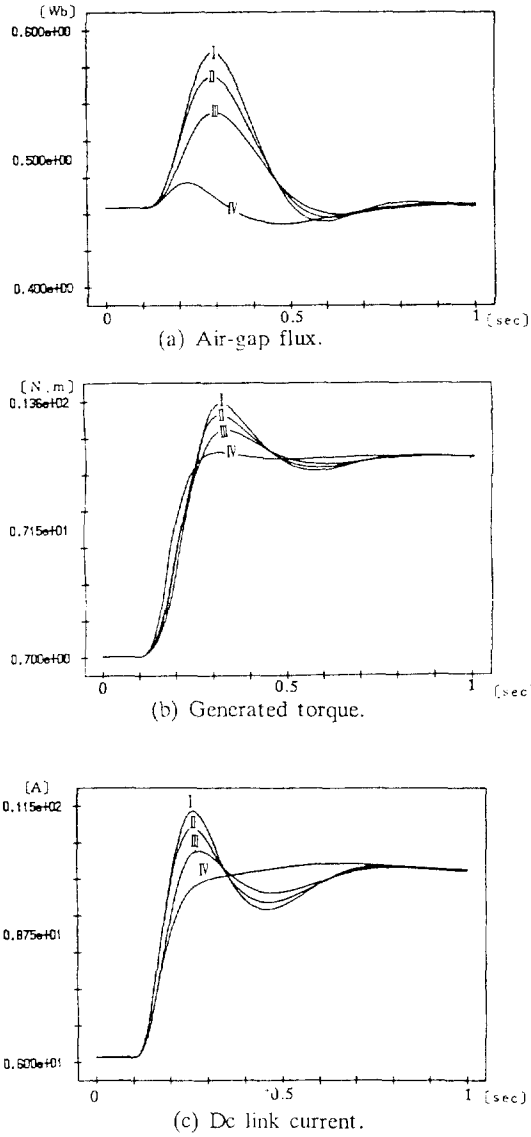


**Fig. 12** Dynamic characteristics(I. SRCI without angle control, II. SRCI with compensation of the inverter time delay $T_d$ only, III. ASCI without angle Control, IV. SRCI with angle control, at $\omega_{ref}$=30Hz $T_l$ : from 0 N.m to 10 N.m).

experiment. Oscillograms of the dc link current and rotor speed for abrupt load torque are also shown in Fig. 13 and Fig. 14, respectively. In these cases, the speed of the induction motor was 600 r / min

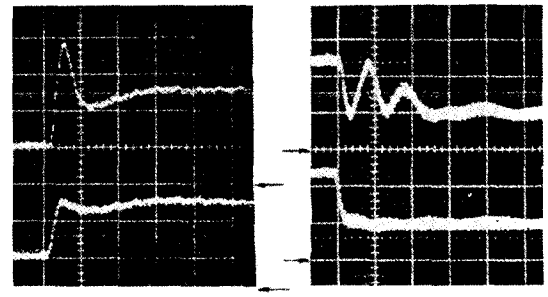


**Fig. 13** Oscillograms of step responses of dc link current for abrupt load torque 0.7pu input. (upper : no compensation, lower : with compensation) 5A / div, 0.2sec / div, → : GND.

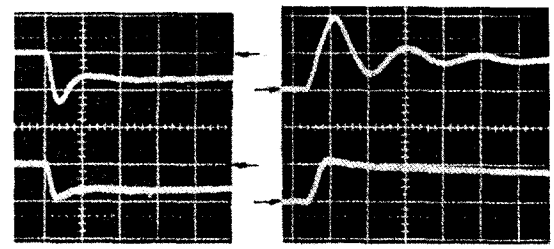


**Fig. 14** Oscillograms of step responses of rotor speed for abrupt load torque of 0.7pu input.(upper : no compensation, lower : with compensation) 60rpm / div, 0.2sec / div, → : 600rpm.

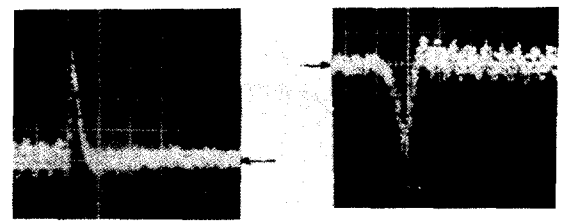


**Fig. 15** Oscillograms of step responses of compensation frequency $d\theta_{eq}$ / dt for abrupt load torque of 0.7pu input 1 Hz / div, 0.1sec / div, → : OHz.

and the magnitude of step load torque change was 0.70 pu. The upper trace of each oscillogram corresponds to without angle control loop and the lower trace coresponds to with angle control loop, respectively. Fig. 13 shows that the overshoots of the dc link current are reduced and the system responses are considerably improved comparing with no compensation. In particular, when the load torque is released, the effects are more obvious of compensation frequency $d\theta_{eq} / dt$. As shown in the oscillograms, the angle control has a dominant effect especially on the transient response of the system.

## 7. Conclusions

The angle control method for recently developed SRCI inverter is proposed. Angle compensation is achieved by considering two terms influcnced by the torque varation and inverter time delay. The amount of torque angle variation is the same for all kinds of the current source inverters, however, the time delay effect is different depending on the inverter types. Complete analysis and computer simulation for these effects are given in this paper. By applying the angle control technique to the SRCI induction motor drive, good dynamic response and large phase margin are obtained. It is shown that the angle control has a dominant effect especially on the transient response of the system, which is verified through the experiment. The improvement of the dynamic response is thought to be due to the nearly constant air-gap flux during the transient interval of load torque change.

## REFERENCES


1) K.P. Phillips, "Current Source Converter for a Motor Drives", IEEE Trans. Ind. Appl., vol.IA-8, no.6, pp.679-683, Nov. / dec 1972
2) R. Krishnan, etc., "Design of Angle Controlled Current Source Inverter-fed Induction Motor Drives", IEEE Trans. IA, vol.IA-19, no.3, May / June 1983.
3) Loren H. Walker, "A High Performance Controlled- Current Inverter Drive", IEEE Trans. Ind. Appl., vol.IA-16, no.2 Mar. / Apr. 1980.
4) Gyu. H. cho, Sun. S. Park, "A New GTO Current Source Inverter with Simultaneous Recovery and Commutation", IEEE international conference, 1986.
5 Edward P. Cornel, etc., "Modeling and Design of Controlled Current Induction Motor Drive Systems", IEEE Trans. IA, vol.IA-13, no.4, July / June 1977.